



Novel broad-spectrum inhibitors of bacterial methionine aminopeptidase



Jonathan A. Rose^a, Sushmita D. Lahiri^b, David C. McKinney^b, Rob Albert^b, Marshall L. Morningstar^b, Adam B. Shapiro^b, Stewart L. Fisher^b, Paul R. Fleming^{b,*}

^a Cleveland Clinic Lerner College of Medicine of Case Western Reserve University, 9500 Euclid Ave., Cleveland, OH 44195, USA

^b Infection Innovative Medicines Unit, AstraZeneca R&D Boston, 35 Gatehouse Drive, Waltham, MA 02451, USA

ARTICLE INFO

Article history:

Received 13 April 2015

Revised 20 May 2015

Accepted 22 May 2015

Available online 30 May 2015

Keywords:

Antibacterial

Methionine aminopeptidase

Azepinone

Structure-based design

Drug discovery

ABSTRACT

With increasing emergence of multi-drug resistant infections, there is a dire need for new classes of compounds that act through unique mechanisms. In this work, we describe the discovery and optimization of a novel series of inhibitors of bacterial methionine aminopeptidase (MAP). Through a high-throughput screening campaign, one azepinone amide hit was found that resembled the native peptide substrate and possessed moderate biochemical potency against three bacterial isozymes. X-ray crystallography was used in combination with substrate-based design to direct the rational optimization of analogs with sub-micromolar potency. The novel compounds presented here represent potent broad-spectrum biochemical inhibitors of bacterial MAP and have the potential to lead to the development of new medicines to combat serious multi-drug resistant infections.

© 2015 Elsevier Ltd. All rights reserved.

Bacterial protein translation has been an abundant source of antibacterial targets including many different classes of drugs that treat serious clinical infections. With resistance to currently prescribed antibiotics increasing, however, there is a need for new classes of compounds that inhibit novel biochemical targets. In prokaryotic organisms, protein translation is initiated with a formylmethionine residue, which is converted to methionine during protein elongation by the metalloenzyme, peptide deformylase (PDF).¹ Inhibitors of PDF containing metal chelating moieties have shown *in vivo* efficacy, however concerns of toxicity remain.² An important step in the co- or posttranslational protein maturation is hydrolysis of the N-terminal methionine by the metalloenzyme, methionine aminopeptidase (MAP).^{3,4} MAP is a ubiquitous enzyme found in all prokaryotes and gene deletion studies have shown it to be essential for *Escherichia coli*⁵ and *Salmonella typhimurium*.⁶ Our own unpublished gene deletion studies have confirmed this essentiality in *Streptococcus pneumoniae* and *Haemophilus influenzae* (data not shown). Therefore, MAP is a validated target for the development of broad-spectrum antibacterial drugs with a novel mechanism of action that could provide therapeutic options to combat multidrug-resistant bacterial pathogens.⁷

There are two major types of MAP enzymes. Type I enzymes are found in eubacteria, while both type I and II enzymes are found in

eukaryotes.⁸ In humans, type I and, in particular, type II MAP have been considered as oncology targets, and type II MAP is known to be inactivated by the anti-angiogenesis compound fumagillin.⁹ This compound and its subsequent analogs have been found to inhibit both endothelial cell growth as well as tumor growth *in vivo*.¹⁰ Similarity of human type I MAP to bacterial MAP is moderate (30–40%), with even lower similarity observed for the type II MAP (20%). Engineering selectivity for bacterial MAP should be achievable given this sequence divergence and the fact that crystal structures of both human¹¹ and bacterial¹² MAP enzymes have been published.

MAP's enzymatic hydrolysis of native proteins requires the assistance of divalent metal ions that serve as a cofactor for the catalytic reaction. MAP activation has been accomplished with Co(II), Mn(II), Ni(II), and Fe(II).¹³ Although several MAPs were initially

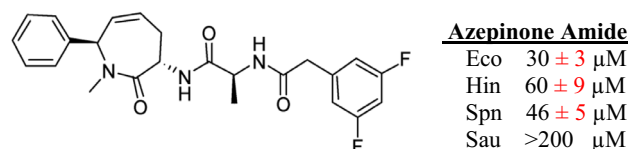
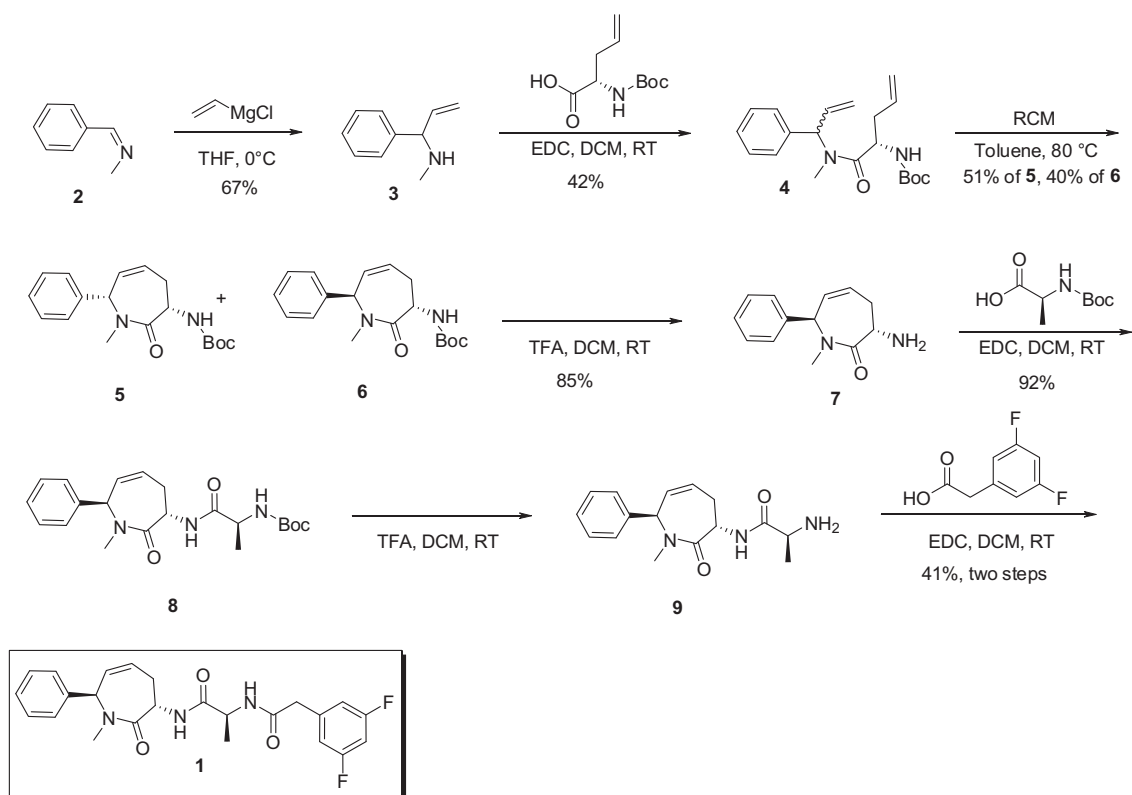


Figure 1. High throughput screen azepinone amide hit (1). Resynthesis of the HTS hit confirmed moderate biochemical activity against three MAP isozymes. Eco = *E. coli*. Hin = *H. influenzae*. Spn = *S. pneumoniae*. Sau = *S. aureus*.

* Corresponding author. Tel.: +1 617 248 5291; fax: +1 617 502 5291.

E-mail address: paulrobertfleming@gmail.com (P.R. Fleming).



Scheme 1. Synthesis of azeponone amide hit (1).

Table 1
Structure–activity relationship of azeponone analogs

Compound number	Structure	Eco IC ₅₀ (μM ± SE)	Hin IC ₅₀ (μM ± SE)	Spn IC ₅₀ (μM ± SE)
10		8.1 ± 1	11.3 ± 1	7.4 ± 1
11		>200	>200	>200
12		>200	>200	>200
13		>200	>200	>200
14		>200	>200	>200
15		>200	>200	>200
16		>200	>200	>200
17		102 ± 18	132 ± 27	71.4 ± 13

IC₅₀ values are best-fit values ± standard error (SE).

identified as Co(II) enzymes, later work has led to the discovery of inhibitors that can target the Co(II)-, Mn(II)-, and Fe(II)-forms of *E. coli* MAP with high potency and selectivity.^{14,15} The inhibitors of Fe(II)-MAP have been shown to be the only ones capable of bacterial growth inhibition against *E. coli* and *Bacillus* strains, suggesting that Fe(II) may be the physiologically relevant metal in MAP.¹⁶ However, because the physiological metal cofactor has not been determined conclusively there is a risk that potent inhibitors of one metalloform may not inhibit other metalloforms and/or translate to in vivo efficacy. One potential strategy for avoiding this difficulty would be to find inhibitors that do not interact directly with the divalent metal but interact solely with the protein amino acid residues. In addition, by forgoing metal chelation as a strategy for inhibition of MAP, concerns about selectivity versus other important human metalloenzymes such as matrix metalloproteinases could potentially be minimized.

In this work, we describe an early drug discovery campaign that led to the identification of a novel chemical series that inhibits multiple bacterial MAP isozymes. We have obtained an X-ray crystal structure of one of these inhibitors bound to the MAP active site, which shows close interactions with the protein without interacting directly with the divalent cation cofactor.

The project began with a high throughput screen (HTS) of over 1.2 million compounds from AstraZeneca's corporate compound collection using a novel high-throughput absorbance-based assay for methionine published previously,¹⁷ in which Mn(II) was used as the metal cofactor. A triage cascade was utilized that was based on progressively more stringent criteria for hits. Over 1000 compounds were tested for purity analysis and inhibition of enzyme activity against *E. coli* MAP. From this set of actives, over 400 compounds were tested for potency against MAP isozymes from *H. influenzae*, *S. pneumoniae*, and *Staphylococcus aureus*. Of these only one chemical series emerged with moderate potency against three of the isozymes (Fig. 1). This hit contained an azepinone amide backbone and resynthesis of the compound confirmed inhibition of enzyme activity. Monocyclic and bicyclic azepinones have been incorporated as dipeptide mimics in mercaptoacyldipeptides inhibitors of angiotensin converting enzyme (ACE)^{18–20} including the marketed ACE inhibitor benazepril.^{21,22} Medicinal chemistry effort was subsequently deployed to achieve potency and physical property optimization.

The synthesis of compound **1** was achieved in 6 steps from **1** commercially available methyl imine starting material (**2**) according to Scheme 1. Grignard reaction with commercially available vinyl magnesium chloride gave the allyl amine (**3**). Amide coupling with EDC and commercially available carboxylic acid was used to form the Boc-protected amide (**4**). Ring-closing metathesis (RCM) was performed in toluene at 80 °C to afford a mixture of isomers that were purified by column chromatography to give a decent yield of the desired azepinone (**5**). Removal of the Boc-protecting group with TFA in dichloromethane at room temperature was then followed by amide coupling using EDC and commercially available Boc-protected-(S)-alanine to generate the ala-Boc azepinone intermediate (**8**). Removal of the Boc-protecting group with TFA in dichloromethane at room temperature and amide coupling with EDC and difluorobenzyl carboxylic acid gave the final compound (**1**) in good yield.

Various azepinone analogs were synthesized in order to explore the series' structure–activity relationship (SAR). Table 1 summarizes the results of efforts to optimize enzyme inhibition and physical properties of the hit compound. Testing of ala-Cbz intermediate (**10**) resulted in a slight improvement in potency as compared to the original hit, which showed that the RHS could be varied to other lipophilic moieties. This also allowed comparative Cbz analogs to be synthesized in fewer steps, enabling rapid SAR generation. Synthesis of left-hand side (LHS) and right-hand

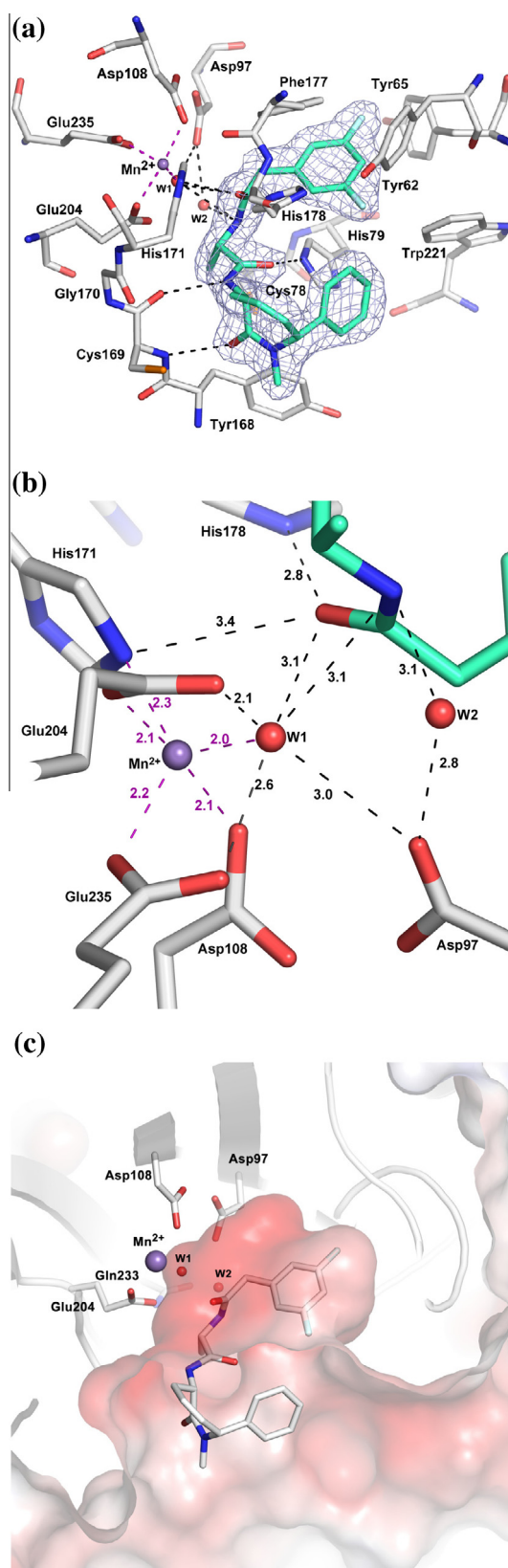


Figure 2. X-ray crystal structure of compound **1** in *E. coli* MAP. (a) There are several strong polar interactions including hydrogen bonds with His79, Cys169, His171 and His178 and indirect interaction with active site residues Asp97, Asp108, Glu235, and Glu204 through a water bridge (W1), which is more clearly shown in (b). The compound does not displace the primary metal, but instead interacts indirectly through W1. (c) The electrostatic surface of the binding pocket shows the positioning of the difluorobenzyl group deep within the hydrophobic pocket and the bent conformation placing the two aromatic rings in close proximity.

side (RHS) fragments (compound **11** and **12**, respectively) showed that both sides of the original backbone are required for enzyme inhibition. LHS modification to compound **13** showed that the *R*-stereochemistry of the phenyl substituent was required for potency. Modifications of the amide linker also resulted in loss of inhibition, including changing to the *gem*-dimethylamino acid **14**, removal of the amide hydrogen to give tertiary amide **15**, and change to include a bulky side chain like valine **16**. Interestingly, an intermediate side chain such as in serine analog **17** allowed for retention of modest potency, likely reflecting a steric constraint in that region of the binding pocket. All analogs demonstrated aqueous solubility >200 μM with other physical properties of certain analogs similar to **1** (see [Supplementary material](#)).

An X-ray crystal structure of **1** in complex with *E. coli* MAP was obtained at 1.8 angstrom resolution (PDB ID 4Z7M). The structure showed one metal bound to the active site and a clear density for compound **1** was in the vicinity (Fig. 2a). Several strong interactions were observed between **1** and the peptide backbone, with no direct interaction with the divalent metal cofactor. However, the compound does not displace the primary metal, but instead interacts with the water molecule that is bound to the metal (Fig. 2b). There are multiple polar interactions observed in the structure. The alanine carboxy oxygen was found to form a hydrogen bond with His79. The amino group of the azepinone ring made a hydrogen bond with the carboxy oxygen of Cys169 and the carboxy oxygen of the azepinone ring made a hydrogen bond with the backbone amide of Cys169. The carboxy oxygen of the benzyl amide formed hydrogen bonds with the imidazole nitrogens of His171 and His178, while the nitrogen of the benzyl amide formed an indirect interaction with active site residues Asp97, Asp108, Glu235 and Glu204 through a water bridge (W1). These interactions are summarized in Figure 2a.

In addition to the polar interactions, there are also hydrophobic residues that contribute to the binding mode. Most notable is the benzyl ring interactions that are positioned in a pocket formed by aromatic residues Phe177, Trp221, Tyr65, and Tyr62. This pocket positions the N-terminal methionine that allows recognition and cleavage of this amino acid, and thus is hydrophobic and enclosed (Fig. 2c). In contrast, the LHS azepinone ring is more solvent exposed, as this part of the pocket binds to the rest of the peptide chain with very little specificity for the amino acid sequence other than the backbone peptide. As a result, there are

limited specific interactions to the LHS group other than to the backbone peptide. However, the outer lining of this pocket is formed of aromatic groups such as Tyr168, Trp221, and Tyr62, which provides favorable interactions to the phenyl substituent of the LHS. Additionally, the structure clearly shows that the inhibitor binds to the pocket in a bent conformation such that the phenyl group of LHS is brought in close proximity to the difluorobenzyl ring of RHS. An intramolecular hydrophobic contact provides some favorable interactions to the otherwise exposed phenyl group of the RHS.

As shown in the crystal structure, the nitrogen of the benzyl amide is shown to be interacting with active site residues Asp97, Asp108, and Glu204 through a water bridge W1 (Figs. 2a and 3a). These residues are theorized to interact with the nitrogen of methionine at the N-terminus of the natural substrate, allowing proper stabilization for peptide hydrolysis.^{13,23} Therefore it was hypothesized that the inhibitor resembles a substrate analog and that addition of a benzyl amino group to the right-hand side would mimic the methionine nitrogen. It was hypothesized that this would result in improved potency through displacement of the water molecule and direct hydrogen-bonding with these three active site residues (Fig. 3b). Consistent with this hypothesis, synthesis of compound **18** showed improved biochemical potency in all three isozymes with sub-micromolar potency against *S. pneumoniae* (Table 2). A small library of benzyl amine compounds showed consistent improvement in potency as compared to the methylene analogs, and delivered the most active compound for this series (**22**) with sub-micromolar inhibition against *E. coli* and *S. pneumoniae* (Table 2). Unfortunately even with this improved potency, compounds **10**, **18**, **21**, and **22** failed to show antibacterial activity at concentrations up to 64 $\mu\text{g/ml}$ against any of the diverse collection of Gram-negative and Gram-positive pathogens in our typical screening panel.

The structural modifications were able to improve biochemical potency against *E. coli* and *S. pneumoniae* MAP, thus allowing the design of a broad spectrum compound. However, the compounds always lacked measurable *S. aureus* potency. Crystal structures of *S. aureus* MAP are available in the public domain and provide a basis for rationalizing this difference. When the *E. coli* structure bound to compound **1** was overlaid on a previously-published *S. aureus* MAP structure (1QXZ, Oefner et al),²⁴ it was clear that all key polar interactions and the residues surrounding the

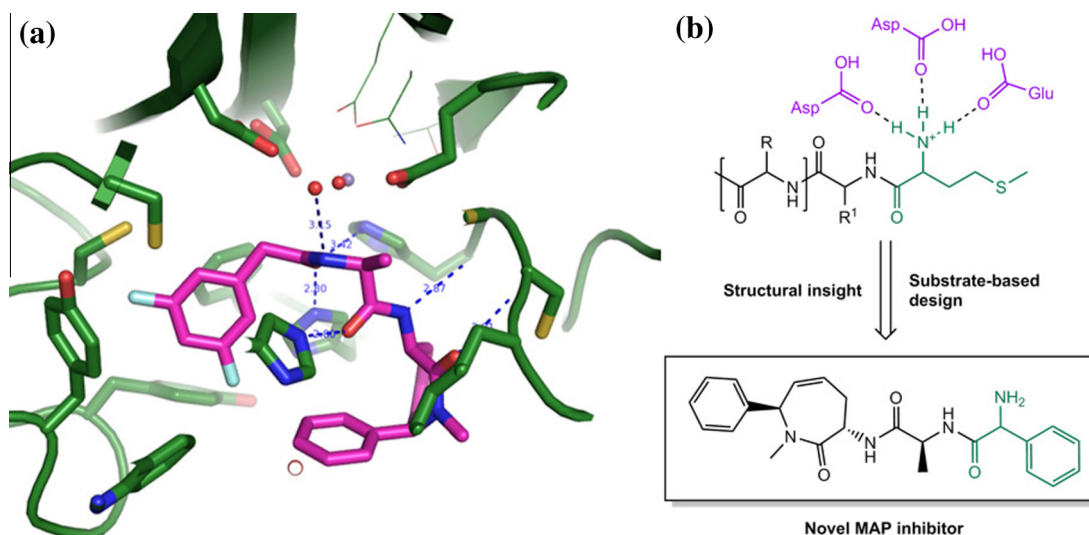


Figure 3. Structure/substrate-based design. (a) X-ray crystal structure of compound **1** in *E. coli* MAP showing interaction of the benzyl amide nitrogen with Asp97, Asp108, Glu235 through a water bridge. (b) Substrate-based design of lead compound hypothesizing that addition of a benzyl nitrogen would mimic the methionine nitrogen of the natural substrate and interact directly with active site residues.

Table 2
Structure–activity relationship of benzyl amine analogs

Compound number	Structure	Eco IC ₅₀ (μM ± SE)	Hin IC ₅₀ (μM ± SE)	Spn IC ₅₀ (μM ± SE)
18		1.4 ± 0.3	6.7 ± 0.7	0.12 ± 0.01
19		8.0 ± 0.9	15.6 ± 1.0	4.0 ± 0.4
20		>200	>200	>200
21		2.2 ± 0.4	4.7 ± 0.5	9.7 ± 1
22		0.8 ± 0.1	1.1 ± 0.1	0.3 ± 0.03

IC₅₀ values listed as mean concentration ± standard error (SE).

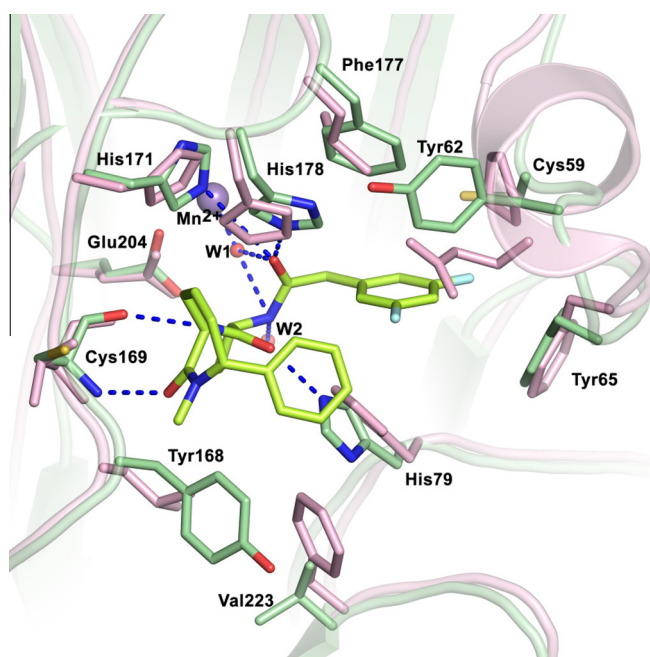


Figure 4. X-ray crystal structure of compound 1 in *E. coli* MAP (green) overlaid with *S. aureus* MAP (pink). The larger helix in the *S. aureus* structure creates a smaller binding pocket for the RHS and may explain the lack of comparable binding potency.

compounds were conserved (Fig. 4). While the amino acids interacting with the LHS moiety were not exactly same, the nature of the substitution, such as Tyr168 replaced with Leu, or Val223 replaced with Phe, remained unchanged and thus would be expected to have minimal impact on binding potency. Interestingly however, the benzyl pocket of the RHS was slightly different in *S. aureus* compared to that of *E. coli*. The residues Cys59, Tyr62, and Tyr65 are contributed by a small helix in *E. coli* (H3 helix). This helix is larger in the *S. aureus* structure, and results in a smaller pocket. We propose that the larger helix is suboptimal for the binding of this scaffold to *S. aureus*, as the RHS binding plane would influence the hydrogen bonding with the backbone residues of the molecule.

We have described the discovery of a novel series of MAP inhibitors with broad-spectrum biochemical potency against *E. coli*, *S. pneumoniae*, and *H. influenzae*. High-throughput screening was used to identify potential candidates from a large compound collection. From this screening campaign, one azepinone amide hit was found that resembled the native peptide substrate and possessed moderate biochemical potency against three bacterial isozymes. An X-ray crystal structure was obtained of this compound bound to *E. coli* MAP, which showed several strong polar interactions between the enzyme and compound backbone in addition to many non-specific hydrophobic interactions. Most notably this structure showed no direct interaction between the compound and divalent metal cofactor. Rational medicinal chemistry and substrate/structure-based design using this crystal structure along with an understanding of MAP's mechanism allowed for the synthesis of compound analogs with sub-micromolar potency. Although *S. aureus* inhibition was never achieved with this series, structural analysis revealed an explanation for this difference in binding affinity and could direct future programs to achieve potency against *S. aureus*. The compounds presented here represent novel MAP inhibitors with the potential to lead to the development of new medicines to treat serious multi-drug resistant infections.

Acknowledgments

Kanayo Azogu, Bridget Reaney, Nancy DeGrace, Ying Liu, Ziling Lu, Camil Joubbran and Mark Zambrowski are thanked for analytical support. Frank Kilty is thanked for bioinformatics support.

Supplementary data

Supplementary data (experimental details and spectroscopic characterization of compounds involved in the synthesis, including ADME characterization of select compounds) associated with this article can be found, in the online version, at <http://dx.doi.org/10.1016/j.bmcl.2015.05.061>.

References and notes

- Solbiati, J.; Chapman-Smith, A.; Miller, J. L.; Miller, C. G.; Cronan, J. E., Jr. *J. Mol. Biol.* **1999**, *290*, 607.
- Jain, R.; Chen, D.; White, R. J.; Patel, D. V.; Yuan, Z. *Curr. Med. Chem.* **2005**, *12*, 1607.

3. Giglione, C.; Boularot, A.; Meinnel, T. *Cell Mol. Life Sci. CMLS* **2004**, *61*, 1455.
4. Bradshaw, R. A.; Brickey, W. W.; Walker, K. W. *Trends Biochem. Sci.* **1998**, *23*, 263.
5. Chang, S. Y.; McGary, E. C.; Chang, S. J. *Bacteriol.* **1989**, *171*, 4071.
6. Miller, C. G.; Kukral, A. M.; Miller, J. L.; Movva, N. R. J. *Bacteriol.* **1989**, *171*, 5215.
7. Vaughan, M. D.; Sampson, P. B.; Honek, J. F. *Curr. Med. Chem.* **2002**, *9*, 385.
8. Arfin, S. M.; Kendall, R. L.; Hall, L.; Weaver, L. H.; Stewart, A. E.; Matthews, B. W.; Bradshaw, R. A. *Proc. Natl. Acad. Sci. U.S.A.* **1995**, *92*, 7714.
9. Sin, N.; Meng, L.; Wang, M. Q.; Wen, J. J.; Bornmann, W. G.; Crews, C. M. *Proc. Natl. Acad. Sci. U.S.A.* **1997**, *94*, 6099.
10. Yin, S.-Q.; Wang, J.-J.; Zhang, C.-M.; Liu, Z.-P. *Curr. Med. Chem.* **2012**, *19*, 1021.
11. Liu, S.; Widom, J.; Kemp, C. W.; Crews, C. M.; Clardy, J. *Science* **1998**, *282*, 1324.
12. Lowther, W. T.; Orville, A. M.; Madden, D. T.; Lim, S.; Rich, D. H.; Matthews, B. W. *Biochemistry (Mosc.)* **1999**, *38*, 7678.
13. Lowther, W. T.; Matthews, B. W. *Chem. Rev.* **2002**, *102*, 4581.
14. Ye, Q.-Z.; Xie, S.-X.; Huang, M.; Huang, W.-J.; Lu, J.-P.; Ma, Z.-Q. *J. Am. Chem. Soc.* **2004**, *126*, 13940.
15. Wang, W.-L.; Chai, S. C.; Huang, M.; He, H.-Z.; Hurley, T. D.; Ye, Q.-Z. *J. Med. Chem.* **2008**, *51*, 6110.
16. Chai, S. C.; Wang, W.-L.; Ye, Q.-Z. *J. Biol. Chem.* **2008**, *283*, 26879.
17. Shapiro, A. B.; Gao, N.; Thresher, J.; Walkup, G. K.; Whiteaker, J. J. *Biomol. Screening* **2011**, *16*, 494.
18. Robl, J. A.; Cimarusti, M. P.; Simpkins, L. M.; Brown, B.; Ryono, D. E.; Bird, J. E.; Asaad, M. M.; Schaeffer, T. R.; Trippodo, N. C. *J. Med. Chem.* **1996**, *39*, 494.
19. Addla, D.; Jallapally, A.; Kanwal, A.; Sridhar, B.; Banerjee, S. K.; Kantevari, S. *Bioorg. Med. Chem.* **2013**, *21*, 4485.
20. Jallapally, A.; Addla, D.; Bagul, P.; Sridhar, B.; Banerjee, S. K.; Kantevari, S. *Bioorg. Med. Chem.* **2015**.
21. Yu, L.-T.; Huang, J.-L.; Chang, C.-Y.; Yang, T.-K. *Mol. Basel Switz.* **2006**, *11*, 641.
22. Maschio, G. et al. *N. Engl. J. Med.* **1996**, *334*, 939.
23. Ye, Q.-Z.; Xie, S.-X.; Ma, Z.-Q.; Huang, M.; Hanzlik, R. P. *Proc. Natl. Acad. Sci. U.S.A.* **2006**, *103*, 9470.
24. Oefner, C.; Douangamath, A.; D'Arcy, A.; Häfeli, S.; Mareque, D. *J. Mol. Biol.* **2003**, *332*, 13.